Available online at www.sciencedirect.com
ScienceDirect
Bioorganic & Medicinal Chemistry Letters 16 (2006) 6277–6280
Bioorganic & Medicinal Chemistry Letters

3D QSAR studies of AChE inhibitors based on molecular docking scores and CoMFA

Nagaraju Akula,[a,b] Laurent Lecanu,[a,b,*] Janet Greeson[c] and Vassilios Papadopoulos[a,b]

[a]*Department of Biochemistry and Molecular Biology, Georgetown University Medical Center, Washington, DC 20057, USA*
[b]*Samaritan Research Laboratories, Georgetown University Medical Center, Washington, DC 20057, USA*
[c]*Samaritan Pharmaceuticals, Las Vegas, NV 89109, USA*

Received 21 July 2006; revised 25 August 2006; accepted 7 September 2006
Available online 16 October 2006

Abstract—Three-dimensional quantitative structure–activity relationship (3D QSAR) studies were performed on acetylcholinesterase (AChE) inhibitors, based on molecular docking scores obtained by using FlexX and FlexiDock and comparative molecular field analysis (CoMFA). The docking scores were used as molecular descriptors along with the steric and electrostatic field values of CoMFA, for partial least square (PLS) analysis. The high leave one out (LOO) cross-validated correlation coefficient ($q_2 = 0.714$) reveals that the model is a useful tool for the prediction of test set as well as newly designed structures against AChE activity. The superimposed CoMFA models on the receptor site of AChE are guiding the design of potential inhibitory structures directed against AChE activity.

Alzheimer's disease (AD), a neurodegenerative disease affecting the elderly population throughout the world, is clinically characterized by an impairment of cognitive function. Aside from the two hallmarks of the disease—the formation of amyloid plaques and neurofibrillary tangles—the main histological change that occurs in the AD brain is the loss of basal forebrain cholinergic neurons, which is associated with reduced cortical and hippocampal levels of acetylcholine and its associated enzyme choline transferase. One possible approach to treat this disease is to restore acetylcholine levels by inhibiting acetylcholinesterase (AChE) with reversible inhibitors.[1–4] Clinical trials have shown that AChE inhibitors such as physostigmine, donepezil, rivastigime, and galantamine effectively improve memory in some patients.[5–12] Designing novel core structures for AChE inhibition is an area of active research in AD. Recently, it has been reported that bis-tacrine congeners display enhanced inhibitory activity toward AChE compared to tacrine, the prototype of this structural family and the first drug marketed for AD treatment.[13–15] Bis-tacrine compounds bind not only to the catalytic site, but also to the AChE peripheral site, and thus, may possibly prevent AChE from promoting Aβ fibrillization.[16–18] In the current study, we have performed 3D QSAR studies by molecular docking and comparative molecular field analysis (CoMFA),[19] which may serve as a useful tool to gain insight into the mechanism of inhibition and to predict the inhibitory properties of newly designed compounds. The results obtained from these studies were superimposed on the active and peripheral receptor sites of AchE, and the ligand–protein interactions were studied. The main focus of the current study was the peripheral site since it contains a number of amino acid residues surrounding the key residue W286. The purpose of this work was to validate and predict the accuracy of biological IC_{50} values of small molecules against AChE by using molecular docking scores and comparative molecular field analysis in combination. We believe that this procedure will be helpful in the design of novel AchE inhibitory compounds.

Computational methodology. All of the ligand structures were built on the basis of the extracted coordinates (3,8-diamino-6-phenyl-5-[6-[1-[2-[(1,2,3,4-tetrahydro-9 acridinyl)amino]ethyl]-1H-1,2,3triazol-4-yl]hexyl]-phenanthridinium) from the reported crystal structure 1Q84.[20] These structures were minimized in Sybyl with Gasteiger charges, and additional minimization was performed

Keywords: QSAR; CoMFA.
* Corresponding author. Tel.: +1 202 687 4625; fax: +1 202 687 2354; e-mail: ll55@georgetown.edu

0960-894X/$ - see front matter © 2006 Elsevier Ltd. All rights reserved.
doi:10.1016/j.bmcl.2006.09.030

with MOPAC using the AM1 method. The optimized structures and MOPAC charges were used for all subsequent calculations. The X-ray crystal structure of the AChE mouse model was obtained from the Brookhaven Protein Data Bank (entry 1Q84). Residue A128 was replaced by Ser to reproduce the rat AChE active site sequence, and these coordinates were used for molecular docking studies to calculate the docking scores using FlexX and Flexidock algorithms (Tripos, St. Louis, MO). These programs were interfaced with Sybyl 7.0 and were used for docking of all of the bis-tacrine compounds at the AchE active site. The active site was defined as including all atoms within a 7.0 Å radius of the co-crystallized ligand. The docking scores (D-Score, G-Score, Chem-Score, and PMF-Score) of the ligands were calculated from the FlexX docked ligand–protein complexes using Cscore.[21–26] In the FlexiDock study, the backbone conformation of residues in the binding pockets of the enzyme was kept rigid while a few rotatable bonds of the ligands were kept flexible to explore the most biologically active conformation. Docking studies were performed for 5000 generations, and only the energetically favorable complexes/conformations were analyzed. On the basis of the ligand orientation, one complex structure for each ligand was selected as the best fit, and its score was added to the molecular spreadsheet.

CoMFA. A total of 19 bis-tacrine structures selected from the literature were used for CoMFA.[16] The training set was made up of 16 structures, and the remaining three structures constituted the test set. Molecular alignment was carried out with the field-fit method using Sybyl7.0. The most active compound, **3H**, was used as the template, and the remaining molecules were aligned to it using the basic core of tacrine. The CoMFA fields were generated using sp^3 C atom with a +1 charge as the probe. The region was created automatically, and the default grid spacing (2 Å) was employed, which extended 5.0 Å units in all directions beyond the dimensions of each molecule. Energy cutoff values of 30 kcal/mol were selected for both the electrostatic and steric fields, and the minimum σ value was set to 2.0. Statistical analysis was performed by applying the partial least square (PLS) procedure to the appropriate columns of the CoMFA table and using the standard scaling method (COMFA_STD). The experimental IC_{50} (nM) values were converted into $-\log(IC_{50})$ values (Table 1) and used as the dependent column. Column filtering for the cross-validated and non-cross-validated CoMFA analysis was set to 2.0 and 0.0 kcal/mol, respectively. The optimal number of components was designated such that cross-validated r^2 was maximal and the standard error of prediction (s_{cross}) was minimal.

Results and discussion. The substituted homodimeric tacrine (9-amino-1,2,3,4-tetrahydroacridine) congeners reportedly exhibit strong inhibitory activities against rat AChE and human BChE. In the current study, we examined only the inhibitory activities against AChE using 3D QSAR studies, specifically molecular docking

Table 1. Structural data, experimental (exp) and calculated (calcd) $-\log IC_{50}$ values of bis-tacrine compounds

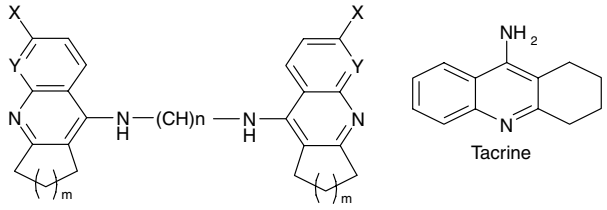

Compound	X	Y	*m*	*n*	$-\log IC_{50}$ (nM)		Residual
					Exp	Calcd	
2A	H	CH	1	6	−2.06	−2.06	0.00
2B	H	CH	1	7	−1.87	−1.81	−0.06
2C	H	CH	1	8	−1.34	−1.39	0.05
3A	H	CH	2	6	−1.04	*−0.52*	*−0.52*
3B	H	CH	2	7	0.69	0.70	−0.01
3C	H	CH	2	8	−0.24	−0.21	−0.03
3D	F	CH	2	6	0.04	−0.03	0.07
3E	F	CH	2	7	0.22	0.31	−0.09
3F	F	CH	2	8	0.15	0.28	−0.13
3G	Cl	CH	2	6	0.22	*0.32*	*−0.1*
3H	Cl	CH	2	7	1.15	1.13	0.02
3I	Cl	CH	2	8	0.52	0.47	0.05
3J	H	N	2	6	−0.68	−0.58	−0.10
3K	H	N	2	7	−0.11	−0.19	0.08
3M	H	N	2	8	−0.27	−0.28	0.01
4A	H	CH	3	6	−0.39	−0.47	0.08
4B	H	CH	3	7	−0.43	−0.44	0.01
4C	H	CH	3	8	−0.2	−0.27	0.07
Tacrine		—	—	—	−2.52	*−1.86*	*−0.66*

The IC_{50} (nM) values have been obtained from Ref. 16. Tacrine and the compounds **3A** and **3G** were not included in the initial set of compounds used to develop the CoMFA model but were used to validate the model (values in italics).

scores and CoMFA. To calculate the docked scores of the inhibitory structures against AChE, we employed the molecular docking programs, FlexX and FlexiDock. FlexX is an automated docking program that assesses ligand conformational flexibility by an incremental fragment placing technique. In the current study, 20 conformational binding modes for each ligand were generated at the active site. All of the 20 conformations were viewed using 3D crystal eyes, and the conformation closest to the crystal structure orientation and with the best score was chosen. It is interesting to note that compounds **3B**, **3E**, and **3I** exhibited better scores than the highly active compound, **3H**. FlexiDock, a genetic algorithm based technique, was used for docking of all the 19 compounds into AChE catalytic active site, and the scores were calculated with the best possible crystal structure orientation/conformation. The results obtained from molecular docking are summarized in Supplementary Table 1.

Compound **3B** exhibited an excellent FlexiDock score among the 19 structures. FlexX and FlexiDocked structures of the **3B** ligand–protein complexes, once aligned and superimposed, clearly showed that, in both cases, one of the tetrahydro acridine moieties of **3B** produces cation-π and π–π interactions with W86 and edge to face interactions with Y449 in the active site region. In addition, the other end of the acridine also forms π–π interactions with W286 at peripheral site (Fig. 1). These results demonstrate the crystal structure orientation of the ligand and confirm the accuracy of the docking and validity of the docking scores for 3D QSAR studies.

The CoMFA model was developed using a training set of 16 compounds listed in Table 1. Tacrine, **3A**, and **3G** were not included in the initial set and defined as test set, so as to test the predictions of the derived CoMFA model. These structures were randomly chosen based on their diverse activities (low, moderate, and high). The AChE binding affinities of the training set, expressed as $-\log IC_{50}$, were related to the independent variables (i.e., steric, electrostatic, and molecular docking scores) using the PLS methodology. The high leave one out (LOO) cross-validated correlation coefficient ($q_2 = 0.714$) revealed that the model is a useful tool for the prediction of AChE inhibitory activity of small molecules. Furthermore, the model yielded a conventional r_2 of 0.97 with a lower standard estimate of 0.082 (Table 2). As an additional test of robustness, the CoMFA model was applied to the excluded ligands—Tacrine, **3A**, and **3G**. The correlation between the actual and predicted activity was fair. In Figure 2a, the steric contour plots of compound 3B are displayed as green contours, which denote regions where an increase in steric bulk would enhance the activity and yellow contours, which indicate regions where an increase in steric bulk would reduce activity.

The large yellow contour situated near the peripheral binding site (nitrogen) suggests that the addition of bulky groups in this region will cause a reduction in activity. Steric bulk groups substituted on the 3rd, 5th, and 6th positions of the cyclohexyl ring toward the active and peripheral sites will improve the activity. A few favorable steric regions were observed close to the C2 aliphatic chain, and small groups or atoms at this position may enhance the activity (Fig. 2a–b). The electrostatic contour plots of compound **3B** are displayed in blue and red contours in Figure 3. The red regions are favorable for electron-rich groups. The blue regions are favorable for electropositive/poor groups and promote inhibitory activity (Fig. 3a). As such, the electropositive nature of the tacrine group at the peripheral site favors an increased activity. The negative charge

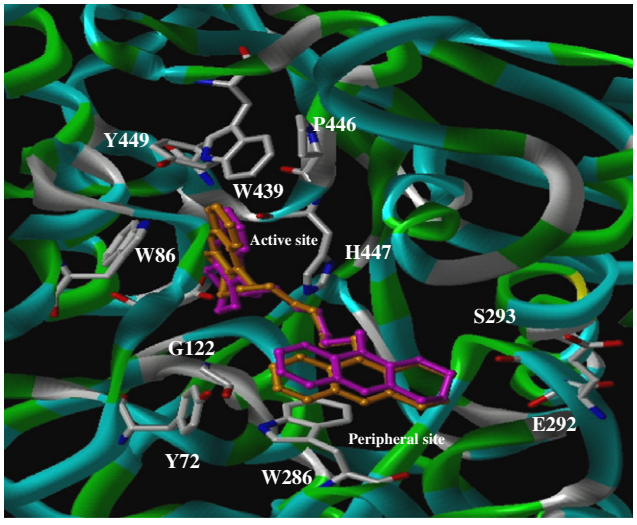

Figure 1. Comparison of the FlexX and FlexiDock, ligand–protein complexes of compound 3B. The bound inhibitor is shown as ball and stick model. Magenta colored ligand is FlexX docked structure where orange color structure is FlexiDock. The backbone of the protein structure is rendered as shaded ribbon with color by property and the labeled protein residues are in capped stick model with color by atom.

Table 2. Statistical analysis of CoMFA

Cross-validate		Conventional		
q^2	No. of components	r^2	SEE	F
0.714	2	0.97	0.082	328.40

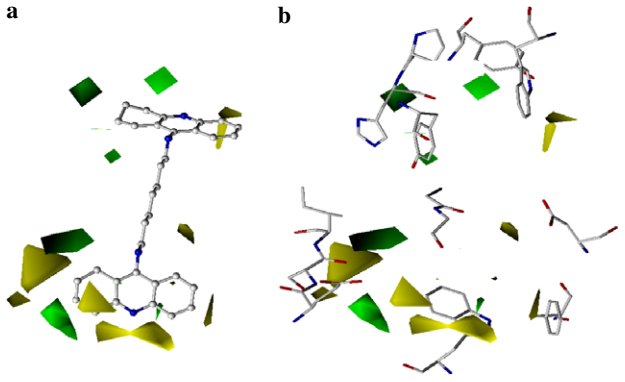

Figure 2. (a) Steric contour plots of compound (b) superimposition of the steric CoMFA contour plot and few active site residues of AChE.

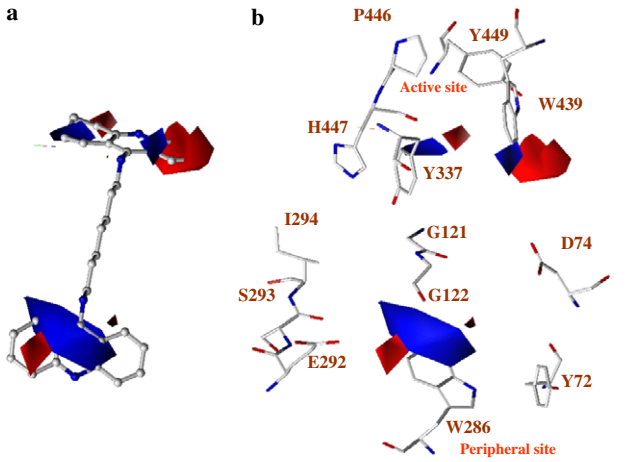

Figure 3. (a) Electrostatic contour plots of compound 3B (b) superimposition of the electrostatic CoMFA contour plot and few active site residues of AChE.

favorable region is observed at the 4th, 5th, and 6th positions of the aromatic ring of bis-tacrine toward the active site region. Electronegative fragments at this position may increase the binding affinity (Fig. 3a–b), and this may account for the high activity of compound **3H**. On the other hand, it should be noted that the addition of electronegative substituents at the 6th position of the cyclohexyl ring might improve the inhibitory activity of the compound. It has been reported that the structure of **3B** was more active than the hetero/homodimeric dichloro substitutes.[27] However, a more recent report showed that the homodimeric mono-chloro substituent, compound 3H, exhibited higher activity than **3B**.[16] Our modeling studies suggest that mono-chloro heterodimeric substituents better occupy the binding site. These modeling studies strongly correlate with the previously reported biological activity data on AchE.

Conclusion. In summary, 3D QSAR analyses have been performed on 19 bis-tacrine compounds using molecular docking scores and CoMFA. A satisfactory CoMFA model was obtained to predict the activities of test set structures. The steric and electrostatic recognition sites of the peripheral binding site as well as the superimposed CoMFA contours on the receptor sites will guide the design of novel structures which demonstrate optimal binding to and inhibition of AchE.

Acknowledgments

We acknowledge the National Cancer Institute for allocation of computing time and staff support at the Advanced Biomedical Computing Center of the National Cancer Institute, Frederick. This work was supported by a contract from Samaritan Pharmaceuticals.

Supplementary data

Supplementary data associated with this article can be found in the online version at doi:10.1016/j.bmcl.2006.09.030.

References and notes

1. Levy, R. *Lancet* **1978**, *2*, 944.
2. Brown, R. C.; Han, Z.; Cascio, C.; Papadopoulos, V. *Neurobiol. Aging* **2003**, *24*, 57.
3. Duffy, L. M.; Hepburn, K.; Christensen, R.; Brugge-Wiger, P. *Image J. Nurs. Sch.* **1989**, *21*, 254.
4. Davila, C.; Viteri, C.; de Castro, P. *Rev. Med. Univ. Navarra* **1997**, *41*, 58.
5. Ballmaier, M.; Casamenti, F.; Scali, C.; Mazzoncini, R.; Zoli, M., et al. *Neuroscience* **2002**, *114*, 91.
6. Barnes, C. A.; Meltzer, J.; Houston, F.; Orr, G.; McGann, K., et al. *Neuroscience* **2000**, *99*, 17.
7. Van Dam, D.; Abramowski, D.; Staufenbiel, M.; De Deyn, P. P. *Psychopharmacology (Berl)* **2005**, *180*, 177.
8. Clegg, A.; Bryant, J.; Nicholson, T.; McIntyre, L.; De Broe, S., et al. *Health Technol. Assess.* **2001**, *5*, 1.
9. Clegg, A.; Bryant, J.; Nicholson, T.; McIntyre, L.; De Broe, S., et al. *Int. J. Technol. Assess. Health Care* **2002**, *18*, 497.
10. Goldlist, B.; Gordon, M.; Naglie, G. *Drugs Aging* **2003**, *20*, 1139.
11. Prasher, V. P. *Int. J. Geriatr. Psychiatry* **2004**, *19*, 509.
12. Snir-Mor, I.; Weinstock, M.; Davidson, J. T.; Bahar, M. *Anesthesiology* **1983**, *59*, 6.
13. Qizilbash, N.; Birks, J.; Lopez-Arrieta, J.; Lewington, S.; Szeto, S. *Cochrane Database Syst. Rev.* **2000**, *3*, CD000202.
14. Pang, Y.-P.; Quiram, P.; Jelacic, T.; Hong, F.; Brimijoin, S. *J. Biol. Chem.* **1996**, *271*, 23646.
15. Carlier, P. R.; Han, Y. F.; Chow, E. S.-H.; Li, C. P.-L.; Wang, H.; Lieu, T. X.; Wong, H. S.; Pang, Y.-P. *Bioorg. Med. Chem.* **1999**, *7*, 351.
16. Hu, M. K.; Wu, L. J.; Hsiao, G.; Yen, M. H. *J. Med. Chem.* **2002**, *45*, 2277.
17. De Ferrari, G. V.; Canales, M. A.; Shin, I.; Weiner, L. M.; Silman, I., et al. *Biochemistry* **2001**, *40*, 10447.
18. Carlier, P. R.; Chow, E. S.; Han, Y.; Liu, J.; El Yazal, J., et al. *J. Med. Chem.* **1999**, *42*, 4225.
19. Cramer, R. D., 3rd; Patterson, D. E.; Bunce, J. D. *Prog. Clin. Biol. Res.* **1989**, *291*, 161.
20. Bourne, Y.; Kolb, H. C.; Radic, Z.; Sharpless, K. B.; Taylor, P., et al. *Proc. Natl. Acad. Sci. U.S.A.* **2004**, *101*, 1449.
21. Bohm, H. J. *J. Comput. Aided Mol. Des.* **1994**, *8*, 243.
22. Eldridge, M. D.; Murray, C. W.; Auton, T. R.; Paolini, G. V.; Mee, R. P. *J. Comput. Aided Mol. Des.* **1997**, *11*, 425.
23. Kramer, B.; Rarey, M.; Lengauer, T. *Proteins* **1999**, *37*, 228.
24. Muegge, I.; Martin, Y. C. *J. Med. Chem.* **1999**, *42*, 791.
25. Muegge, I.; Martin, Y. C.; Hajduk, P. J.; Fesik, S. W. *J. Med. Chem.* **1999**, *42*, 2498.
26. Meng, E. C.; Kuntz, I. D.; Abraham, D. J.; Kellogg, G. E. *J. Comput. Aided Mol. Des.* **1994**, *8*, 299.
27. Savini, L.; Campiani, G.; Gaeta, A.; Pellerano, C.; Fattorusso, C., et al. *Bioorg. Med. Chem. Lett.* **2001**, *11*, 1779.